

Water Content Measurement and Modeling in the Nitrogen + Water System

Amir H. Mohammadi,[†] Antonin Chapoy,[‡] Bahman Tohidi,[†] and Dominique Richon^{*,‡}

Centre for Gas Hydrate Research, Institute of Petroleum Engineering, Heriot-Watt University, Edinburgh EH14 4AS, Scotland, U.K., and Centre Energétique et Procédés, Ecole Nationale Supérieure des Mines de Paris, CEP/TEP, 35 Rue Saint Honoré, 77305 Fontainebleau, France

Experimental data and thermodynamic modeling of water solubility in nitrogen are reported herein. Equilibrium data were measured in the (282.86 to 363.08) K temperature range at pressures up to about 5 MPa using a static-analytic technique taking advantage of a Rolsi sampling device. Two different thermodynamic approaches have been used to represent the new experimental data. The first approach employs the Peng–Robinson equation of state with classical mixing rules and a Henry's law treatment for calculating the fugacities in the vapor and aqueous phases, respectively. The second approach uses the Valderrama modification of the Patel–Teja equation of state with non-density-dependent mixing rules for modeling the fluid phases. The new experimental data are in good agreement with the predictions of the models and some selected experimental data from the literature, demonstrating the reliability of the experimental technique and predictive methods used in this work.

1. Introduction

Natural gases are normally saturated with water in reservoirs. During production, transportation, and processing, the dissolved water in the natural gas may form a condensate, which leads to corrosion or gas hydrates/ice formation. To predict and avoid such problems and also to design and select operating conditions in natural gas and gas injection facilities, accurate knowledge of phase behavior for natural gas main components and water systems over wide temperature and pressure ranges is necessary.

Therefore, experimental data are crucial for successfully developing and validating models capable of predicting the phase behavior of these systems over a wide temperature range.

A preliminary study on the water content of natural gas main components shows a need for generating novel data over a broad range of conditions.¹

In this work, new water content measurements in the vapor (or gas) phase of the nitrogen + water system have been generated in the (282.86 to 363.08) K temperature range for pressures up to about 5 MPa. The different isotherms presented herein were obtained using an apparatus based on a static-analytic method taking advantage of a new kind of Rolsi electromagnetic capillary sampler.² The vapor-phase compositions were measured by a gas chromatography (GC) method.

Two thermodynamic models based on the equality of fugacities of each component throughout all phases are employed to model the phase equilibria. The first thermodynamic approach is based on the Peng–Robinson equation of state (PR-EoS)³ including the classical mixing rules (or van der Waals one-fluid mixing rules) for the vapor phase and a Henry's law approach to treat the aqueous phase using binary interaction parameters (BIPs) adjusted on

previously reported solubility data.⁴ The Valderrama modification of the Patel–Teja equation of state (VPT-EoS)⁵ with the non-density-dependent (NDD)⁶ mixing rules is used in the second approach for predicting the fugacity of components in fluid phases using previously reported BIPs.⁴ To evaluate the consistency of the new data further, the experimental results are compared with other experimental data from the literature. The results are in good agreement, demonstrating the capability of techniques and models used in this work.

2. Experimental Section

2.1. Materials. Helium from Air Liquide was pure grade with traces of water (3 ppm) and hydrocarbons (0.5 ppm). Nitrogen was purchased from Air Liquide with a certified purity of 99.9999 vol %. Deionized water was used after degassing.

2.2. Apparatus. The apparatus used in this work is based on a static-analytic method with vapor-phase sampling, which is similar to that previously described by Chapoy et al.² Measurement uncertainties are estimated to be not higher than ± 0.02 K in the (273.15 to 393.15) K range for temperature and within ± 1 kPa in the (0.2 to 5) MPa range for pressure.

The analytical work was carried out using a gas chromatograph (Varian model CP-3800) equipped with a thermal conductivity detector (TCD) connected to a data acquisition system fitted with Borwin software (version 1.5, from JMBS, Le Fontanil, France). The analytical column is a Hayesep T 100/120 mesh column (silcosteel tube, length 1.5 m, diameter $\frac{1}{8}$ in. from Resteck).

The TCD was utilized to detect both compounds. For nitrogen, it was repeatedly calibrated by introducing known amounts of nitrogen through a gas syringe in the injector of the gas chromatograph. The uncertainties of the calculated moles of nitrogen are estimated to be within $\pm 0.9\%$ in the (4.1×10^{-6} to 2.1×10^{-5}) mol range. Because the water concentration is very low, calibrating the detectors is very difficult. It is indeed impossible to correctly inject

* To whom correspondence should be addressed. E-mail: richon@paris.ensmp.fr. Tel: +(33) 1 64 69 49 65. Fax: +(33) 1 64 69 49 68.

[†] Heriot-Watt University.

[‡] Ecole Nationale Supérieure des Mines de Paris.

such a small quantity in the chromatograph using syringes. For calibration purposes, a dilutor apparatus is used with a specific calibration circuit. The calibration procedure has been previously described in Chapoy et al.^{7,8} and Mohammadi et al.^{1,9} The cell of the dilutor is immersed inside a liquid thermoregulated bath. Helium is bubbled through the dilutor cell filled with water to be saturated before entering the chromatograph through an external loop injection valve. In using the dilutor and a loop injection valve, a well-defined amount of water can be injected into the chromatograph. The calculation of the amount of water, n_2 , is carried out using an equilibrium and mass balance relation^{1,7,8}

$$n_2 = \gamma_2^L x_2^L \frac{P_2^{\text{sat}}}{P_{\text{dilutor}}} \frac{\varphi_2^{\text{sat}}}{\varphi_2^V} \left(\frac{PV}{ZRT} \right)^{\text{loop}} \exp \left(\left(\frac{v_2^L}{RT} \right) (P_{\text{dilutor}} - P_2^{\text{sat}}) \right) \quad (1)$$

where γ_2^L is the activity coefficient of water in the aqueous phase, x_2^L is the mole fraction of water in the liquid aqueous phase of the dilutor, P_2^{sat} stands for the vapor pressure of water at temperature T , P_{dilutor} represents the pressure in the dilutor, φ_2^{sat} is the vapor-fugacity coefficient of saturated pure water, φ_2^V is the vapor-fugacity coefficient of water, P , V , Z , and R are the pressure, volume, compressibility factor, and gas constant, the superscript loop stands for loop properties, and v_2^L is the molar volume of liquid water at T .

It is of essential interest to know the volume and the dead volume of the sampling valve (loop volume + dead volume = V^{loop}) precisely. First, the volume of the external loop is roughly calculated (around 40 μL), and then a calibration with methane (purchased from *Messer Griesheim* with a certified purity greater than 99.995 vol %) as a reference gas using a 50- μL gas syringe is done around the value of the rough estimation. After this careful methane calibration, methane is passed through the sampling valve and injected into the GC. Knowing the number of moles of methane swept into the GC through the previous calibration, we estimate the volume and the dead volume of the loop to be 35.50 $\mu\text{L} \pm 0.09 \mu\text{L}$. The experimental accuracy of the TCD water calibration (from 7.5×10^{-9} to 3.4×10^{-7} mol) is estimated in the worst case to $\pm 4\%$.

2.3. Sampling Devices. The sampling is carried out using a new Rolsi capillary sampler injector. The sampler-injector is connected to the cell through 0.1-mm internal diameter capillary tubing. The withdrawn samples are swept into a Varian 3800 gas chromatograph for analysis. The capillary inlet of the sampler is directly in contact with the vapor phase, and the outlet of the capillary is closed by a movable microstem operated by an electromagnet. When the electromagnet is activated, the outlet of the capillary is opened so that a sample can flow and is mixed with the carrier gas through the expansion room. This expansion room is crossed by the carrier gas, which sweeps the sample to be analyzed into the GC column. The sampler allows direct sampling at the working pressure without disturbing the cell equilibrium because of the relatively small size of the sample. The sample mass can be adjusted continuously from 0.01 to several milligrams thanks to an electronic timer. The expansion room of the sampler is heated independently from the equilibrium cell to allow the samples to remain in the vapor state and eventually vaporize a liquid sample.

2.4. Experimental Procedure. The equilibrium cell and its loading lines are evacuated down to 0.1 Pa prior to introduction of about 5 cm^3 of degassed water. Then,

nitrogen is introduced into the cell directly from the commercial cylinder (through preliminary evacuated transfer lines) to a pressure level corresponding to the pressure of the first measurement. More gas is introduced after each sampling and analysis steps up to given pressures. After each introduction of gas into the cell, efficient stirring is started, and pressure is stabilized within a few minutes; measurements are performed only when pressure is constant within experimental uncertainty. (Furthermore, pressure is verified to be constant all along the sample analyzes.)

For each equilibrium condition, at least 10 samples are withdrawn from the vapor phase using the sampler and analyzed to check for measurement repeatability. Because the volume of the withdrawn samples is very small (typically less than 1 mg) compared to the total mass inside the equilibrium cell (more than 5 g), it is possible to withdraw many samples without significantly disturbing the studied phase equilibrium.

3. Thermodynamic Model

3.1. Pure-Compound Properties. The critical temperature (T_c), critical pressure (P_c), critical volume (v_c), and acentric factor (ω) for each of the pure compounds are provided elsewhere.^{4,10} In this paper, nitrogen and water are labeled as components 1 and 2, respectively.

3.2. First Model. In this approach, an activity coefficient model is used for the condensed aqueous phase, and an equation of state is employed for the vapor phase. At equilibrium, the fugacity of each component must be equal in both phases. The PR-EoS combined with the van der Waals one-fluid mixing rules is employed to calculate fugacities in the vapor phase. The PR-EoS is selected because of its simplicity and its widespread use in chemical/petroleum engineering. The expression of the PR-EoS for a pure compound is

$$P = \frac{RT}{v-b} - \frac{a(T)}{v(v+b) + b(v-b)} \quad (2)$$

where v is the molar volume of the system. Parameters b and $a(T)$ are given by

$$b = 0.07780 \frac{RT_c}{P_c} \quad (3)$$

$$a(T) = a_c \alpha(T) \quad (4)$$

where

$$a_c = 0.45724 \frac{(RT_c)^2}{P_c} \quad (5)$$

and subscript c denotes critical conditions. In this work, we have chosen the generalized alpha function, $\alpha(T)$, proposed by Coquelet et al.¹¹ to have an accurate representation of the vapor pressures of pure compounds:

for $T < T_c$, $\alpha(T) =$

$$\exp \left[c_1 \left(1 - \frac{T}{T_c} \right) \right] \left[1 + c_2 \left(1 - \sqrt{\frac{T}{T_c}} \right)^2 + c_3 \left(1 - \sqrt{\frac{T}{T_c}} \right)^3 \right]^2 \quad (6)$$

$$\text{for } T \geq T_c, \alpha(T) = \exp \left[c_1 \left(1 - \frac{T}{T_c} \right) \right] \quad (7)$$

where c_1 , c_2 , and c_3 are correlated to acentric factor ω

$$c_1 = 1.3569\omega^2 + 0.9957\omega + 0.4077 \quad (8)$$

$$c_2 = -11.2986\omega^2 + 3.5590\omega - 0.1146 \quad (9)$$

$$c_3 = 11.7802\omega^2 - 3.8901\omega + 0.5033 \quad (10)$$

For mixtures, the van der Waals one-fluid mixing rules are applied with classical binary interaction parameters k_{ij} . The expressions for parameters a and b become

$$a = \sum_i \sum_j x_i x_j a_{ij} \quad (11)$$

$$b = \sum_i x_i b_i \quad (12)$$

where

$$a_{ij} = \sqrt{a_i a_j} (1 - k_{ij}) \quad (13)$$

x_i and x_j are the mole fractions of components i and j , respectively. At thermodynamic equilibrium, the fugacities f_i of each component i must be equal in the vapor and liquid phases.

$$f_i^L = f_i^V \quad (14)$$

where superscripts L and V stand for liquid and vapor phases, respectively.

The vapor fugacity comes from

$$f_i^V = \varphi_i^V P y_i \quad (15)$$

where φ_i^V and y_i are the fugacity coefficient and mole fraction of component i in the vapor phase, respectively. For the aqueous phase, a Henry's law approach is used to calculate the solubility of gaseous components in water. Fugacities f_1^L and f_2^L of nitrogen and water in the liquid phase at pressure P and temperature T are given by

$$f_1^L = H_{1,2}^L x_1^L \exp\left[\frac{v_1^\infty}{RT}(P - P_2^{\text{sat}})\right] \quad (16)$$

$$f_2^L = \gamma_2^L \phi_2^{\text{sat}} P_2^{\text{sat}} x_2^L \exp\left[\frac{v_2^{\text{sat}}}{RT}(P - P_2^{\text{sat}})\right] \quad (17)$$

where $H_{1,2}^L$ is the Henry's law constant of nitrogen in the liquid aqueous phase at temperature T , x_1^L and x_2^L are the mole fractions of nitrogen and water in the liquid aqueous phase, v_1^∞ is the partial molar volume of nitrogen at T and infinite dilution, and v_2^{sat} is the molar volume of saturated pure liquid water at T . Because nitrogen is at infinite dilution, the asymmetric convention ($\gamma_1^L \rightarrow 1$ when $x_1^L \rightarrow 0$) is used to express Henry's law for the gas (eq 16), whereas the symmetric convention ($\gamma_2^L \rightarrow 1$ when $x_2^L \rightarrow 1$) is used for water (eq 17). By combining eqs 15 and 16, we get the nitrogen mole fraction x_1^L as

$$x_1^L = \frac{P \varphi_1^V y_1}{H_{1,2}^L \exp\left[\frac{v_1^\infty}{RT}(P - P_2^{\text{sat}})\right]} \quad (18)$$

The fugacity coefficients in the vapor phase are calculated by using the PR-EoS. In this paper, the partial molar volume v_1^∞ is calculated with a general correlation based

Table 1. BIPs for the VPT-EoS and NDD Mixing Rules^a

system	k_{2-1}^a	l_{2-1}^{0b}	$l_{2-1}^1 \times 10^{4b}$
nitrogen + water	0.4788	2.6576	65.1018

^a k_{2-1} : BIP for the classical mixing rules. ^b l_{2-1}^0 and l_{2-1}^1 : constants for the BIP for the asymmetric term.

Table 2. Experimental ($y_{2\text{exptl}}$) and Predicted ($y_{2\text{prd}}$) Water Contents (Mole Fraction) in the Nitrogen (1) + Water (2) System

T/K	P/MPa	$y_{2\text{exptl}} \times 10^4$	model 1		model 2	
			$y_{2\text{prd}} \times 10^4$	AD %	$y_{2\text{prd}} \times 10^4$	AD % ^a
282.86	0.607	20.40	20.20	1.0	20.30	0.5
282.99	1.799	7.14	7.23	1.3	7.24	1.4
282.99	3.036	4.46	4.51	1.1	4.50	0.9
283.03	4.408	3.17	3.29	3.8	3.27	3.2
293.10	0.558	42.50	42.00	1.2	42.60	0.2
293.19	1.828	13.60	13.60	0.0	13.70	0.7
293.10	2.991	8.44	8.61	2.0	8.66	2.6
293.10	4.810	5.58	5.72	2.5	5.73	2.7
304.02	0.578	79.30	77.10	2.8	78.70	0.8
304.36	1.257	37.00	37.00	0.0	37.70	1.9
304.51	2.539	18.80	19.30	2.7	19.60	4.3
304.61	4.638	11.20	11.40	1.8	11.50	2.7
313.30	0.498	153.00	148.00	3.3	152.00	0.7
313.15	1.246	60.90	60.20	1.1	61.60	1.1
313.26	2.836	27.80	28.00	0.7	28.50	2.5
313.16	4.781	17.50	17.50	0.0	17.80	1.7
322.88	0.499	240.00	241.00	0.4	248.00	3.3
323.10	1.420	87.20	88.20	1.1	90.40	3.7
322.93	3.397	39.60	38.70	2.3	39.50	0.3
322.93	4.841	29.20	28.30	3.1	28.80	1.4
332.52	0.461	427.00	414.00	3.0	426.00	0.2
332.45	1.448	134.00	135.00	0.7	139.00	3.7
332.52	2.454	85.50	82.10	4.0	84.30	1.4
332.52	4.358	48.80	48.60	0.4	49.80	2.0
342.31	0.425	719.00	696.00	3.2	718.00	0.1
342.31	0.462	658.00	641.00	2.6	661.00	0.5
342.39	1.466	219.00	208.00	5.0	214.00	2.3
342.42	2.899	103.00	109.00	5.8	112.00	8.7
342.31	4.962	66.60	66.70	0.2	68.40	2.7
351.87	0.540	849.00	822.00	3.2	848.00	0.1
352.12	1.480	335.00	310.00	7.5	320.00	4.5
351.92	2.957	162.00	159.00	1.9	164.00	1.2
351.95	4.797	111.00	102.00	8.1	105.00	5.4
363.00	0.555	1260.00	1240.00	1.6	1280.00	1.6
363.08	4.874	161.00	155.00	3.7	160.00	0.6

^a Absolute deviation AD = $|(y_{2\text{exptl}} - y_{2\text{prd}})/y_{2\text{exptl}}|$.

on the work of Lyckman et al.¹² and reported by Heide-
mann and Prausnitz¹³ in the following form:

$$\left(\frac{P_{c,i} v_i^\infty}{RT_{c,i}}\right) = 0.095 + 2.35 \frac{TP_{c,i}}{c_2' T_{c,i}} \quad (19)$$

where $P_{c,i}$ and $T_{c,i}$ are the critical pressure and critical temperature of gas i , respectively, and c_2' is the cohesive energy density of water

$$c_2' = \frac{\Delta U_2^{\text{vap}}}{v_2^{\text{sat}}} \quad \text{with} \quad \Delta U_2^{\text{vap}} = \Delta H_2^{\text{vap}} - RT \quad (20)$$

where ΔU_2^{vap} and ΔH_2^{vap} are the molar internal energy and the molar enthalpy of vaporization of pure water at T ,

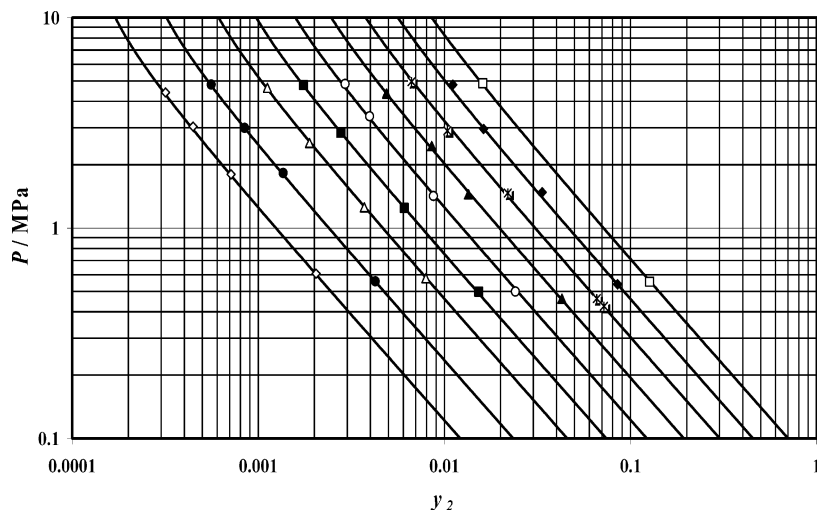


Figure 1. Water content (mole fraction), y_2 , in the vapor phase of the nitrogen + water system: \diamond , 283.0 K; \bullet , 293.1 K; \triangle , 304.4 K; \blacksquare , 313.2 K; \circ , 323.0 K; \blacktriangle , 332.5 K; $*$, 342.3 K; \blacklozenge , 352.0 K; \square , 363.0 K. Solid lines, water content predicted at experimental temperatures with model 1.

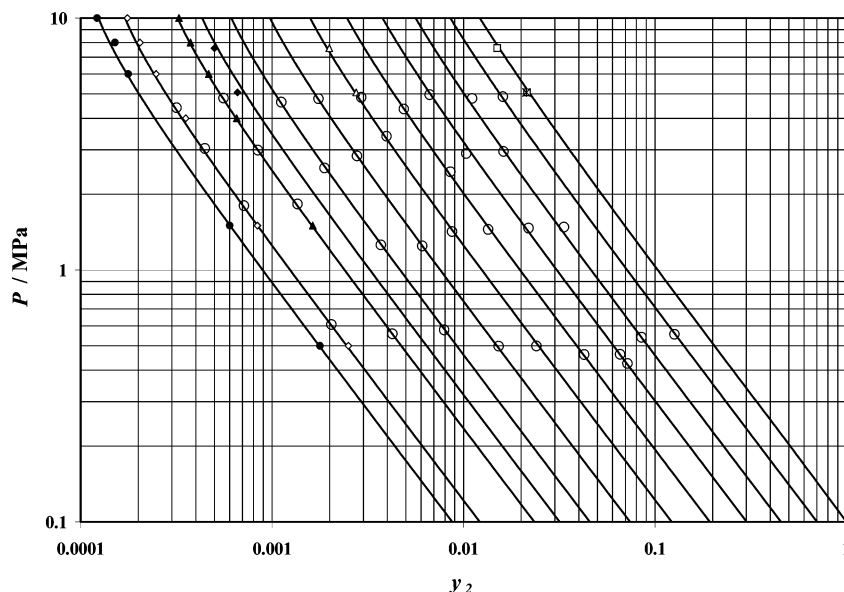


Figure 2. Water content (mole fraction), y_2 , in the vapor phase of the nitrogen + water system: \bullet , 278.15 K from Althaus;²⁰ \diamond , 283.15 K from Althaus;²⁰ \blacktriangle , 293.15 K from Althaus;²⁰ \blacklozenge , 298.15 K from Maslennikova et al.²¹; \triangle , 323.15 K from Maslennikova et al.²¹; \square , 373.15 K from Maslennikova et al.²¹; $*$, 373.15 K from Sidorov et al.;²² \circ , this work. Solid lines, water content calculated at 278.15, 283.15, 293.15, 298.15, 303.15, 313.15, 323.15, 333.15, 343.15, 353.15, 363.15, and 373.15 K with model 1.

respectively. For a better representation of v_i^∞ at high temperatures, we use the following correction

$$v_i^\infty = [v_i^\infty]_{\text{Lyckman et al.}} + \left(\frac{dv_2}{dT}\right)^{\text{sat}} (T - 298.15) \quad (21)$$

where $[v_i^\infty]_{\text{Lyckman et al.}}$ is the partial molar volume of gas (nitrogen) at infinite dilution obtained from eq 19 and T is in K. The Henry's law constants for nitrogen are taken from the literature¹⁴ and are calculated using the following correlation:

$$\log_{10}(H_{1,2}^L(T)) = 78.8622 - \frac{3.74498 \times 10^3}{T} - 24.7981 \times \log_{10}(T) \quad (22)$$

where $H_{1,2}^L$ and T are in atm and K, respectively. The NRTL model¹⁵ is used to calculate water activity coefficient γ_2^L appearing in eq 17.

The BIPs of the first model are adjusted directly to vapor-liquid equilibrium data reported previously.⁴ Adjustments performed on each isotherm independently revealed that BIPs are temperature-independent in the considered temperature range:

$$k_{21} = k_{12} = 0.484$$

where k_{21} and k_{12} are the BIPs for the van der Waals one-fluid mixing rules. To calculate the water activity through the NRTL model, it is recommended that $\tau_{1,2} = 2880 \text{ J}\cdot\text{mol}^{-1}$ and $\tau_{2,1} = 2560 \text{ J}\cdot\text{mol}^{-1}$, and $\alpha_{j,i} = 0.3$ be used (adjustment realized on the previously reported solubility data⁴), where $\tau_{1,2}$, $\tau_{2,1}$, and $\alpha_{j,i}$ represent parameters of the NRTL model.

3.3. Second Model. A thermodynamic model based on the same equation of state for fluid phases that can be used to write the equality of the fugacities of each component throughout the phases^{16,17} is used to model the phase equilibrium. A detailed description of the model for predict-

ing the water content of gases is given elsewhere.¹ Briefly, the VPT-EoS with the NDD mixing rules is employed for these purposes. This EoS–mixing rules combination has proven to be a strong tool in modeling systems with polar and/or nonpolar compounds⁶ and in modeling phase behavior in water–natural gas components system.^{1,2,4,9,18,19} The BIPs between nitrogen–water are set to those reported previously⁴ and are listed in Table 1.

4. Results and Discussion

The new experimental water content data are reported in Table 2 and are plotted in Figure 1. Our isothermal P , y data sets are well represented by the first approach. The agreement between the experimental (exptl) and predicted (prd) data is good, with typical AD (absolute deviation AD = $|y_{2\text{exptl}} - y_{2\text{prd}}|/y_{2\text{exptl}}$) values between 0.0 and 8.1%.

These data are also compared with the predictions of the second thermodynamic model. The agreement between the experimental and predicted data is good, with typical AD values between 0.1 and 8.7%. The AAD (average absolute deviation AAD = $(1/N)\sum^N(|y_{2\text{exptl}} - y_{2\text{prd}}|/y_{2\text{exptl}})$, where N is the number of experimental points, among all of the experimental and predicted data is 2.4% for the first model and 2.0% for the second model. For further evaluation, a comparison is also made between the new data and some selected data from the literature. The results for all conditions are consistent with those of all the authors, as illustrated in Figure 2. The agreement between the new experimental data, predictions of both thermodynamic models, and the selected literature data demonstrates the reliability of the experimental data, technique, and predictive methods used in this work.

5. Conclusions

New experimental data on the water content of the nitrogen + water system were generated in the (282.86 to 363.08) K temperature range and for pressures up to about 5 MPa using a static-analytic apparatus, taking advantage of a high-pressure capillary sampler. The new experimental data were compared with predictions of two previously reported thermodynamic models and some selected experimental data from the literature. Good agreement was achieved, demonstrating the reliability of the experimental data and technique and the predictive methods used in this work.

Literature Cited

- (1) Mohammadi, A. H.; Chapoy, A.; Richon, D.; Tohidi, B. Experimental measurement and thermodynamic modeling of water content in methane and ethane systems. *Ind. Eng. Chem. Res.* **2004**, *43/22*, 7148–7162.
- (2) Chapoy, A.; Mohammadi, A. H.; Tohidi, B.; Richon, D. Water content measurement and modeling for methane + water and methane + ethane + *n*-butane + water systems using a new sampling device. Submitted to *J. Chem. Eng. Data*, 2004.
- (3) Peng, D.-Y.; Robinson, D. B. A new two constant equation of state. *Ind. Eng. Chem. Fundam.* **1976**, *15/1*, 59–64.
- (4) Chapoy, A.; Mohammadi, A. H.; Tohidi, B.; Richon, D. Gas solubility measurement and modeling for nitrogen + water system from 274.18 K up to 363.02 K. *J. Chem. Eng. Data* **2004**, *49/4*, 1110–1115.
- (5) Valderrama, J. O. A generalized Patel-Teja equation of state for polar and nonpolar fluids and their mixtures. *J. Chem. Eng. Jpn.* **1990**, *23/1*, 87–91.
- (6) Avlonitis, D.; Danesh, A.; Todd, A. C. Prediction of VL and VLL equilibria of mixtures containing petroleum reservoir fluids and methanol with a cubic EoS. *Fluid Phase Equilib.* **1994**, *94*, 181–216.
- (7) Chapoy, A.; Coquelet, C.; Richon, D. Solubility measurement and modeling of water in the gas phase of the methane/water binary system at temperatures from 283.08 to 318.12 K and pressures up to 34.5 MPa. *Fluid Phase Equilib.* **2003**, *214*, 101–117.
- (8) Chapoy, A.; Coquelet, C.; Richon, D. Measurement of the water solubility in the gas phase of the ethane + water binary system near hydrate forming conditions. *J. Chem. Eng. Data* **2003**, *48/4*, 957–966.
- (9) Mohammadi, A. H.; Chapoy, A.; Tohidi, B.; Richon, D. Measurements and thermodynamic modeling of vapor-liquid equilibria in ethane–water systems from 274.26 to 343.08 K. *Ind. Eng. Chem. Res.* **2004**, *43/17*, 5418–5424.
- (10) Avlonitis, D. A. Multiphase equilibria in oil–water hydrate forming systems; M. Sc. Thesis, Heriot-Watt University, 1988.
- (11) Coquelet, C.; Chapoy, A.; Richon, D. Development of a new alpha function for the Peng–Robinson equation of state: Comparative study of alpha function models for pure gases (natural gas components) and water – gas systems. *Int. J. Thermophys.* **2004**, *25/1*, 133–158.
- (12) Lyckman, E. W.; Eckert, C. A.; Prausnitz, J. M. Generalized reference fugacities for phase equilibrium thermodynamic. *Chem. Eng. Sci.* **1965**, *20*, 685–691.
- (13) Heidemann, R. A.; Prausnitz, J. M. Equilibrium data for wet-air oxidation. Water content and thermodynamic properties of saturated combustion gases. *Ind. Eng. Chem. Proc. Des. Dev.* **1977**, *16/3*, 375–381.
- (14) Yaws, C. L.; Hopper, J. R.; Wang, X.; Rathinsamy, A. K.; Pike, R. W. Calculating solubility & Henry's law constants for gases in water. *Chem. Eng.* **1999**, June, 102–105.
- (15) Renon, H.; Prausnitz, J. M. Local compositions in thermodynamic excess functions for liquid mixtures. *AIChE J.* **1968**, *14*, 135–144.
- (16) Avlonitis, D. A. Thermodynamics of gas hydrate equilibria; Ph.D. Thesis, Heriot-Watt University, 1992.
- (17) Tohidi, B.; Burgass, R. W.; Danesh, A.; Todd, A. C. Hydrate inhibition effect of produced water, Part 1. Ethane and propane simple gas hydrates. *SPE 26701, Proceedings of the SPE Offshore Europe 93 Conference* **1993**, 255–264.
- (18) Chapoy, A.; Mohammadi, A. H.; Richon, D.; Tohidi, B. Gas solubility measurement and modeling for methane – water and methane – ethane – *n*-butane – water systems at low-temperature conditions. *Fluid Phase Equilib.* **2004**, *220*, 113–121.
- (19) Chapoy, A.; Mokraoui, S.; Valtz, A.; Richon, D.; Mohammadi, A. H.; Tohidi, B. Solubility measurement and modeling for the system propane-water from 277.62 to 368.16 K. *Fluid Phase Equilib.* **2004**, *226*, 213–220.
- (20) Althaus, K. *Fortschritt – Berichte VDI* **1999**, Reihe 3, 350. (in German), Oelrich, L. R.; Althaus, K. GERG – Water correlation (GERG Technical Monograph TM14) relationship between water content and water dew point keeping in consideration the gas composition in the field of natural gas. *Fortschritt – Berichte VDI* **2000**, Reihe 3- Nr. 679 (in English).
- (21) Maslennikova, V. Ya.; Vdovina, N. A.; Tsiklis, D. S. Solubility of water in compressed nitrogen. *Russ. J. Phys. Chem.* (Zh. Fiz. Khim.: In Russian) **1971**, *45/9*, 1354.
- (22) Sidorov, I. P.; Kazarnovsky, Y. S.; Goldman, A. M. *Tr. Gosudarst. Nauch.-Issled. I. Proekt. Inst. Azot. Prom.* **1953**, *1*, 48 (Data from Dortmund Data Base).

Received for review September 9, 2004. Accepted December 21, 2004. The financial support of the European Infrastructure for Energy Reserve Optimization (EIERO) provided the opportunity for this joint work, which is gratefully acknowledged.

JE049676Q